Coating of Rh/Mg/Al Hydrotalcite-Like Materials on FeCrAl Fibers by Electrodeposition and Application for Syngas Production

Coating of Rh/Mg/Al hydrotalcite-like materials on FeCrAl fibers by electrodeposition and application for syngas production

*Phuoc Hoang Ho, Francesca Ospitali, Giancosimo Sanghez De Luna, Giuseppe Fornasari, Angelo Vaccari, and Patricia Benito**

Dr. P. H. Ho, Dr. F. Ospitali, G. Sanghez De Luna, Prof. G. Fornasari, Prof. A. Vaccari, and Prof. P. Benito
Dipartimento di Chimica Industriale "Toso Montanari", Università di Bologna, Viale Risorgimento 4, 40136, Bologna, Italy
E-mail: * patricia.benito3@unibo.it
Keywords: structured catalyst, electrodeposition; hydrotalcite, FeCrAl fibers, catalytic partial oxidation of methane

Metallic fibers are promising supports to develop structured catalysts due to high thermal stability, mechanical strength and geometrical surface area. However, such a high surface area is usually associated with small individual fibers and tiny pores, leading to pore blockage during coating process. Herein, the electrodeposition as a simple way to deposit Rh/Mg/Al hydrotalcite-like materials on FeCrAl fibers is investigated. Several trials are performed to optimize the synthesis conditions in the electro-base generation method using nitrates as precursors, focusing on total metal nitrate concentration and synthesis time. A combination of the two parameters is screened to find a balance between coating, quality and loading. A low electrolyte concentration (e.g. < 0.06 M) required longer synthesis time to obtain an appropriate loading without pore blockage, whereas a high concentration (e.g. 0.10 M) may cause the deposition of undesired Rh^0 particles. Tailoring the solid loading and decreasing the cracks in the electrodeposited samples result in a quite stable coating during a further thermal treatment step to transform hydrotalcite-like compounds into oxide- and spinel-based catalysts. All the tested catalysts are active in the catalytic partial oxidation of methane at GHSV of 351,000 h^{-1}, although their catalytic activities significantly depend on the coating properties.

1. Introduction

The catalytic partial oxidation (CPO) of methane to synthesis gas or syngas (CO + H_2) is an attractive process for natural gas or biogas conversion. This process requires very short contact times (millisecond) and gives rise to high yields in syngas with a H_2/CO ratio close to 2, an ideal feedstock for methanol production or Fischer-Tropsch synthesis. These low contact times allow to achieve a large throughput with a small reactor size, and hence improve the dynamic response of the process making the CPO of methane an industrial option for syngas production, [1-4] especially in remote locations where available sources of methane are abundant. [5] However, in this very fast and exothermic reaction, a large amount of heat inside the catalytic bed and pressure drop are generated. The former gives a challenging task to control heat balance as well as catalyst sintering due to hotspot formation, while the latter decreases the energetic efficiency of the process. The issues of the CPO could be addressed by using structured catalysts that offer advantages in comparison to conventional pelletized ones.

The advantages of structured catalysts such as large geometrical surface area, high void fraction to decrease the pressure drop, enhancement for heat/mass transfer, and process intensification are recently summarized in some reviews.[6-8] Rh-based materials are the most common choice for the development of structured catalysts because it is highly active in the CPO of CH_4.[5] Moreover, in structured catalysts, usually a thin layer of active material is needed to reach a high process efficiency due to large geometrical surface area and enhanced mass transfer. In the other words, the use of a low amount of Rh in the development of structured catalysts may balance its high cost. Various structured supports have been used for the preparation of noble metal-based structured catalysts for the CPO of CH_4, i.e. honeycomb monolith,[9-12] open-cell foam,[13-17] or wire mesh.[18] Fiber-based structured supports provide high bed porosities with large interfacial area, which are promising for applications in fast, mass transfer limited catalytic processes.[19] However, few works use metallic fibers,[20, 21]

although they are applied for other catalytic processes, e.g. dry reforming [22, 23] and combustion/oxidation.[24-26]

Depending on manufacturing technologies, fiber properties (e.g. fiber diameter and bed porosity) can be flexibly varied, thus reaching trade-offs between mass transfer and pressure drop that limit conventional packed bed reactors. Though it may happen that there is no intrinsic difference between mass transfer and pressure drop properties of fiber-based supports and packed beds due to the pore blockage during the coating procedure.[27] It means that for the fiber-based structured supports, it is important to find a compatible coating method that prevents clogged coating material to avoid an increase of pressure drop.

To date, fiber-based structured catalysts (also wire-mesh supports) are prepared by coating techniques such as wash-/dip-coating, in situ precipitation, spray coating, autocatalytic plating, galvanic deposition, which are summarized in detail by Reichelt and co-workers.[28] These techniques are also common for the preparation of other structured catalysts such as honeycomb monolith or open-cell foams.[7, 29] Conventional wash-coating/dip-coating, originally developed for ceramic substrates, is more challenging for metallic ones due to large dissimilarity of thermal expansion coefficients between coating materials (usually ceramic properties) and the metallic structured supports. In addition, for fiber structured support, the use of wash-coating route (dealing with deposition of a viscous slurry and removal of excess material after coating) may increase the risk of pore blockage. Therefore, investigating an alternative to wash-coating procedure is still attractive for the development of fiber-based structured catalysts.

In the last decade, the electro-base generation method has been proposed by us as an efficient method to coat open-cell metallic foams, especially those with small pores. Either hydrotalcite-like or cerium-based materials are successfully electrodeposited on FeCrAl or NiCrAl open-cell foams, which are then transformed into structured catalysts by calcination and used for energy and environmental applications.[16, 17, 30-34] Herein, we further extend the

use of electrodeposition for the coating by Rh/Mg/Al hydrotalcite-like compounds of fibers as precursors of structured catalysts. The electrochemical properties of the fiber substrate are investigated to determine the suitable applied potential controlling the base-generation by reduction of both nitrate and water. Several trials are performed modifying the concentration of the Rh/Mg/Al nitrate electrolytes and the synthesis time to tailor both solid loading and reduce the formation of cracks. The final aim is to obtain stable coatings after a further thermal treatment step to transform hydrotalcite-like compounds into oxide- and spinel-based catalysts. The performances of the structured catalysts are evaluated in the catalytic partial oxidation of CH_4 at a high Gas Hourly Space Velocity (GHSV) value of 351,000 h^{-1}. The dependence of catalytic activity on coating properties is investigated to propose. This work proposes the electrodeposition as an alternative to dip-coating for the preparation of structured catalysts based on metallic fiber supports.

2. Results and Discussion

2.1. Physico-chemical and electrochemical properties of FeCrAl fiber

The fiber support used in this study was made of a FeCralloy. **Figure 1** displayed SEM images and Raman spectra of the fresh and calcined bare fiber. The fiber disc consisted of individual fibers with an average diameter of 20 – 25 μm (**Figure 1a**). Surface of fresh fiber was quite smooth, though some small nodes were observed (**Figure 1b**). EDS showed that these spots had an Al-rich composition. Additionally, impurities containing Zr and Hf were also identified in some locations. From Raman analyses, the peaks at 810 and 850 cm^{-1} that appeared in some spectra were probably due to the presence of chromates (**Figure 1c**).[35] Additionally, weak bands at about 1380 and 1590 cm^{-1} due to carbonaceous species were also detected, in agreement with the 10 – 25 mol% of C identified by EDS (not shown). It is

noteworthy that this C content is much higher than that in FeCrAl open-cell foam used in our previous work, in which C was present only in traces as ι-carbide ($Cr_{23+x}Fe_xC_6$).[17]

Insert Figure 1.

After calcination at 900 ºC for 12 h, whiskers typical of an alumina scale were observed on the surface of the fiber (**Figure 1d and 1e**). In addition, other oxide phases were also identified by Raman. In **Figure 1f** peaks at 297, 415, 613, 1050, and 1610 cm^{-1} were related to Fe_2O_3 [36], those at at 510 and 668 cm^{-1} attributed to $Fe_3O_4/FeCr_2O_4$,[37, 38] while the bands at 350 and 555 cm^{-1} together with those at around 297 and 613 cm^{-1}, possibly overlapped with Fe_2O_3 aforementioned, were related to Cr_2O_3.[35] Analogously to fresh fibers, some carbon-related bands observed at 1380 to 1610 cm^{-1} were probably associated to iron carbides, although its content decreased to around 3 – 6 mol.% during thermal treatment.

Understanding the electrochemical behavior of the substrates during electrodeposition is of paramount importance to tailor the deposition parameters. The electrodeposition method is based on the generation of OH^- by reduction of nitrates, although water reduction could also occur. The latter, however, may negatively influence the stability of the coating due to formation of H_2 bubbles. To investigate the electrochemical activity of the fiber support in the reduction of water and nitrates in absence or presence of cations being precipitated, several LSVs were performed at the fibers immersed in different electrolytes as reported in our previous works,[39, 40] and the results are displayed in **Figure 2**.

Insert Figure 2

With KCl and KNO_3 electrolytes, the onset potentials of the LSVs were around – 1.1 V and -0.9 V, respectively. The cathodic currents were due to water reduction in the former, and to both nitrate and water reduction in the latter. The differences in the current generated in KCl and KNO_3 electrolytic solutions were not large as the cathodic potential increased. For instance, at -1.1 V when water started to be reduced, the current density was around 50 % larger for KNO_3 than KCl, while it was 47 and 36% larger at -1.2 and -1.4 V, respectively.

The presence of cations being precipitated such as Mg^{2+} and Al^{3+} shifted the onset potentials to less cathodic values than the -0.9 V obtained in KNO_3, e.g. about -0.7 V for both 0.0675 M $Mg(NO_3)_2$ and 0.045 M $Al(NO_3)_3$ solutions. However, further increasing the potential to more cathodic values than the onset one, the current increased more rapidly in the $Al(NO_3)_3$ than that in the $Mg(NO_3)_2$ solution, suggesting that Al^{3+} sped up the reduction processes more than Mg^{2+} ions. A 0.06 M mixed solution Mg/Al-NO_3 (Mg/Al = 3/1 as atomic ratio or a.r.) showed similar initial cathodic reduction potential and generated a current density in between those generated by single-cation containing solutions.

With open-cell foams, it was reported that under similar experimental conditions (electrolytes and electrochemical techniques) the nitrates were reduced mainly to nitrites NO_2^- in KNO_3 solution or further to NH_4^+ in a mixed solution of $Mg(NO_3)_2$ and $Al(NO_3)_3$; the reduction of nitrates significantly accounted for OH^- generation and hence increase of pH near to the foam surface.[39] Herein the electrochemical performances of fiber and open-cell foam supports were compared considering the onset cathodic potential and the contribution of nitrate reduction. The onset potentials observed in KCl and KNO_3 solutions were similar to those on FeCrAl open-cell foams.[39, 40] In addition, the rates of current increases were quite similar; for instance, in KCl solution the current values at -1.2 V were 122 and 125% higher than those at -1.1 V for fiber and foam, respectively. While in KNO_3 solutions the current values at -1.2 V increased more 110 and 95% than those at -1.1 V for fiber and foam, respectively. The contribution ratio of water reduction was calculated as the ratio of the current density of water reduction (in KCl solution) and total reduction of water and nitrate (in KNO_3 solution). These ratios at -1.2 V were 53 and 12% for fiber and foam, respectively. In other words, nitrate reduction contribution to total reduction (water and nitrate) was around 47% at fiber and 88% at foam. These results suggest that the fiber was less active than the foam in the nitrate reduction, making more challenging their coating by electrodeposition.

The onset potentials shifted to lower values when including Rh^{3+} ions in the Mg^{2+}/Al^{3+} electrolyte (around -0.5 V vs -0.7 V), namely using the electrolyte for the synthesis of the catalysts. The increase of the total metal concentration led to an increase in the current density (**Figure 2b**), similar to that observed for FeCrAl open-cell foam.[39, 40]

2.2. Catalyst prepared in Rh/Mg/Al 0.06 M electrolytic solution

Taking advantage of our experience in the preparation Rh/Mg/Al hydrotalcite-like compounds on open-cell foams, some trials were performed in electrolytic solutions with total metal nitrate concentration of 0.06 M at -1.2 V. SEM images of samples prepared in the time range from 250 to 1000 s are shown in **Figure 3**.

At 250 s, the fiber was well coated by a compact layer without any pore blockage (**Figure 3a and 3a1**). However, the thickness was quite thin, about 1 – 2 µm (**Figure 3a2**), resulting in a low solid loading (ca. 1.0 wt.%). Prolonging the synthesis time to 500 s, more material was deposited with a loading of 1.2 wt.%., this leads not only to an increase of layer thickness, but also to the numbers of cracks (**Figure 3 b – b2**). Further prolonging the time to 750 and 1000 s, solid loadings increased to 2.2 and 2.5 wt.%, respectively (**Figure 3c and 3d**). At 1000 s, the thickness, estimated within the cracks, was around 10 – 12 µm (**Figure 3d2**). In these four samples, the typical morphology of the particles in the coatings was spherical (inset **Figure 3b2**). In some locations near the support surface, platelet-like particles were also observed (inset **Figure 3c2**), characteristic of the coating on open-cell foams.[32] It should be noted that at these deposition conditions (0.06 M and -1.2 V), synthesis times longer than 1000 s caused severe pore blockage, due to smaller pores in the fibers than in the foams.

Insert Figure 3

The composition of the deposits (Rh/Mg/Al a. r.) was estimated from EDS analyses, and the results are presented in **Figure S1**. Among the three elements (Rh, Mg, Al), Al signal may come both from the coating and the fiber substrate. Therefore, to gain more accurate results, the compositions were obtained from measurements in thick layers (**Figure S1d**), where the

signals of Fe and Cr coming from the substrate alloy were negligible, or in a piece of solid detached (**Figure S1a**). For all the samples, the average composition was approximately Rh/Mg/Al = 4.2/61.7/34.1 (a.r), quite close to the nominal one in the electrolyte. However, for the sample prepared at 1000 s, the formation of some layers rich in Rh and Al laying on the top of the coating (or outer layer) were found in some places. These phenomena were already observed in previous works on FeCrAl open-cell foams,[16, 40, 41] and they were related to the ineffective replenishment of the solution near the substrate surface as well as the formation of an insulating layer during the electrodeposition. Since this work used a double-compartment electrochemical flow cell providing a circulation of the electrolyte during the synthesis, the issue of an ineffective replenishment may be probably ruled out.[32]

Therefore, the presence of an outer layer could be related to a low electrical conductivity and hence to a lower activity in the nitrate reduction of the fibers than the foams due to the C-rich composition identified by aforementioned EDS analyses. This issue was probably more pronounced with an increase of insulating layer during the synthesis. In fact, such effect of low electrical conductivity of the support on the control of the coating composition was reported for NiCrAl open-cell foam, in which a synthesis without removing the oxide layer on the support surface resulted in a coating of Rh- and Al-rich layer.[42]

Insert Figure 4

To transform the hydrotalcite-like precursors into the catalysts, the coated fibers were calcined at 900 ºC for 12 h in a static oven. Stability of the coating layers was evaluated by SEM analyses and the results are shown in **Figure 4**. After thermal treatment, the thin and compact layer of sample deposited in 250 s was still stable without significant crack formation (**Figure 4a**). High magnification images show that the spherical morphology of the coating was not largely modified (**Figure 4a1**). For the coatings prepared at longer synthesis times, the solid films were still well-adhered, although the number of cracks slightly increased after thermal treatment (**Figure 4b, c, and d**). Two kinds of morphologies were clearly

identified: spherical particles on the deposits, which were stable like the particles in the sample prepared at 250 s; and whiskers in the crack near the fiber surface due to alumina formed by calcination of the fiber (**Figure 4 b1, c1, and d1**). Indeed, the same morphology was also observed when a bare fiber was calcined under the same conditions (**Figure 1e**)

In summary, the deposition in a 0.06 M electrolytic solution for short time (250 s) resulted in a compact and highly stable coating even after thermal treatment, while prolonging the electrodepositions (500, 750, and 1000 s) increased in the number of cracks. However, the former also resulted in low loading of the catalytic active phase. A balance between quality of the coating and its loading should be reached in order to obtain a better catalytic activity of the fiber.

To improve the coating quality, another strategy was approached by using either lower or higher metal nitrate concentration in the electrolyte solution. Firstly, four trials with combination of two variables, namely concentration (0.03 or 0.05 M) and time (750 or 1000 s) were performed. SEM images of the electrodeposited and calcined samples are displayed in **Figure 5 and 6**, respectively. In the 0.03 M electrolyte, the coatings were compact regardless of the deposition time (**Figure 5a, a1, b, and b1**). Especially, at 1000 s, although the loading was 1.9 wt.%, close to that of sample at 0.06 M and 750 s above described, the coating was improved and it showed less cracks. Increasing the concentration to 0.05 M resulted in slightly higher solid loadings, 2.0 and 2.1 wt.% for 750 and 1000 s, respectively. The quality of the coating improved with less cracks in comparison to films prepared in 0.06 M electrolytes (**Figure 5c, c1, d, and d1**).

Insert Figure 5 and Figure 6

After calcination at 900 °C for 12 h, although some cracks developed, the coating was stable and well-adhered to the fibers (**Figure 6**). The morphology was not largely modified in comparison to the samples before calcination. The formation of the alumina protective scale from the fiber was scarcely observed.

A further increase of total concentration of the electrolytes to 0.1 M reduced significantly the limitation of nitrate and cation mass transport from bulk solution to the fiber surface and hence a higher cathodic current was measured as shown in **Figure S2**. This resulted in a significant increase in the amount of coating even at short synthesis times. The loadings were 2.3, 3.1, and 4.4 wt.% for depositions at 250, 350, and 500 s, respectively. It is noteworthy that 4.4 wt.% loading at 500 s was almost two times the value deposited in 0.05 M at 1000 s or in 0.06 M at 750 s. However, such high loading also resulted in an increase of cracks, even at a very short deposition time as 250 s (**Figure 7 a1, b1, and c1**). The number of cracks increased when prolonging the synthesis time to 500 s. In some locations with cracks, the estimated thickness was around 6-10 μm. High magnification SEM images showed a spherical morphology (**Figure 7 a2, b2, and c2**). The composition of all the samples at this concentration was close to the nominal one (Rh/Mg/Al = 4.5/67.6/27.8 a.r.) in almost all the regions of interest investigated (**Figure S3 a, b, and c**). However, in some cases Rh^0 particles were also found, which were formed during the electrodeposition, especially in samples prepared at long time, e.g. at 500 s (inset **Figure 7 c1**).

It is interesting to compare the characteristics of the coatings on fibers with those on open-cell foams reported in our previous works. In open-cell foam coatings, deposited in a 0.10 M electrolyte for 2000 s, Rh^0 particles, Mg-rich- layers and Rh/Al-rich coatings were observed.[16] The first and second species were also observed for the fibers, but not the third one. The absence of the Al-rich layer in the present work could be explained by the much shorter deposition time son fiber (less than 500 s versus 2000 s), differences in geometry and electrochemical properties between fibers and foams, and probably in the electrochemical cell configuration (static single-compartment cell versus double-compartment flow cell).

Insert Figure 7

After calcination at 900 ºC, the coating was partially detached like in as-synthesized samples (**Figure 8a, b, and c**). However, the morphology and size of the catalyst particles were not largely modified by thermal treatment (inset **Figure 8a1, b1, c1**).

Insert Figure 8

2.3. Catalytic activity in the CPO of CH_4

The fiber-based structured catalysts were tested in the catalytic partial oxidation of CH_4 using only one coated fiber disc (10 mm of diameter and 1 mm of thickness). After reduction at 750 ºC for 2 h under H_2/N_2 = 1/1 v/v, first diluted and then concentrated gas mixtures ($CH_4/O_2/N_2$ = 2/1/20 and 2/1/4 v/v) were fed at T_{oven} = 750 ºC and GHSV = 351,600 h^{-1}. At the end of the tests with concentrated feedstock, the reaction was performed again feeding the diluted mixture as a control test to evaluate a possible deactivation/activation of the catalyst. CH_4 conversions obtained by some selected catalysts are presented in **Figure 9,** while average values of CH_4 conversion, selectivity and H_2/CO molar ratio are summarized in **Table 1**.

Insert Figure 9

Insert Table 1

All catalysts investigated showed an increase of activity with time-on-stream in the initial reaction conditions with diluted gas mixture ($CH_4/O_2/N_2$ = 2/1/20 v/v). Thus they suffered by an extra activation period under reaction conditions due to further reduction of hardly reducible Rh^{3+} species once syngas was produced, this is a typical behaviour of Rh/Mg/Al hydrotalcite-derived structured catalysts reported in our previous works.[16, 32] In general, over all the catalysts, conversions with concentrated gas mixtures were higher than those in diluted mixtures from 9 – 16% (Table 1), probably due to contribution of the heat generated by the exothermic reactions.[43] In fact, the temperature (at the inlet) in the concentrated gas mixture was 40-80 ºC higher than that in the diluted mixture, in accordance with the higher conversion of the former.

The catalytic performance significantly depended on the catalyst synthesis conditions, due to modifications in amount and quality of the coating. For example, catalysts prepared at both 0.03 M – 750 s and 0.06 M – 500 s exhibited about 46 % of CH_4 conversion in concentrated gas mixture. Although the coatings on those samples were compact and stable, the low amount of solid deposited limited the catalytic performance. Slightly higher CH_4 conversions in both diluted and concentrated feeds were achieved over the samples with higher solid loadings (samples 0.03 M – 1000 s, 0.06 M – 750 s, and 0.10 M – 250 s).

The role of quality of the coating on the activity was demonstrated by comparison of two samples prepared at 0.05 M – 1000 s and 0.10 M – 500 s. Although the solid loading in the former was almost a half of that on the latter, the coating was more stable and contained less cracks. As a result, the sample prepared at 0.05 M – 1000 s (**Figure 9a**) outperformed the one obtained at 0.10 M – 500 s (**Figure 9b**) in terms of CH_4 conversion and syngas selectivity. This catalyst exhibited CH_4 conversions around 46.4 and 60.8% with diluted and concentrated gas mixture, respectively. Both syngas selectivity (82.2% CO and 54.4% H_2) and H_2/CO ratio (1.32 mol/mol) in the concentrated feed were much higher than those obtained with the other catalysts tested (Table 1). It was also noted that this catalyst was further activated after the tests with concentrated gas mixtures, the conversion of CH_4 in the control tests increased around 4% in comparison to the initial test with the same diluted gas mixture. In addition, the sample prepared at 0.10 M – 500 s exhibited a slight decrease in CH_4 conversion with the concentrated gas mixture (about 2%) and during the control test (about 3%), suggesting that the catalyst was partially deactivated. This might be related to the sintering of Rh^0 particles, which were observed even in the electrodeposited sample, due to the heat generated from the reaction. The control tests also confirmed a slightly deactivation of the sample 0.03 M – 750 s, but quite stable performance for others, e.g. 0.03 M – 1000s, 0.06 M – 750 s, and 0.10 M – 250 s.

It should be highlighted that the tests were performed with only one fiber disc at high GHSV value, 351,000 h^{-1}, calculated by a total flow rate of 460 mL min^{-1} and a volume of 78.5 mm^3, and that referred to WHSV (based on mass of coating) in range of $1.25*10^7$ – $2.76*10^7$ (1.0 – 2.2 mg of coating after calcination, depending on synthesis conditions). These high GHSV value justify the low values of CH_4 conversion and low H_2/CO ratio of syngas. Actually, in the CPO, CH_4 conversion occurs by exothermic and fast total/partial oxidations in the first mm of the catalytic bed and consecutively endothermic steam reforming.[16] Therefore, a low selectivity in H_2 on the fiber disc is probably due to lack of length of the catalytic bed for the "steam reforming zone". This could be further improved in future work by increasing the length of the catalytic bed. In fact, using an open-cell foam coated by the same type of Rh-based hydrotalcite-derived materials, CH_4 conversion and syngas selectivity were over 90%. [32]

2.4. Spent catalysts

The coating may be modified due to harsh reaction conditions such as high GHSV values and temperatures inside the catalytic bed. SEM analysis was used to investigate morphology of the coating of the spent catalysts, and pictures of four selected samples prepared with electrolytes with different total metal concentrations are displayed in **Figure 10**. Compared to the respective calcined samples, the coating remained well adhered, the globular particles were observed in high magnification images (**Figure 10 a2, b2, c2, and d2**).

Insert Figure 10

In order to investigate whether the deposition of carbon on the catalyst or the alteration of the fiber alloy took place under reaction conditions, spent catalysts were analyzed by micro-Raman and the results were shown in **Figure 11**. Carbon formation was evidenced in all the tested samples by bands at 1345 and 1590 cm^{-1}. It should be noted that on the same type of Rh/Mg/Al materials with about 10-fold larger amount of catalyst deposited on open-cell foam showed higher resistance to carbon formation, and the carbon formation depended on the

position along the catalytic bed, being more pronounced in reforming zone rather than oxidation zone (near the inlet stream).[32] Therefore, either a low amount of active catalyst on the disc or thin disc of fiber accounted for carbon formation in all tested fiber catalysts. Further investigation is required to study the stability of fiber catalysts with larger amount of catalyst as well as longer catalytic bed.

Insert Figure 11

3. Conclusions

In the electrodeposition tailoring the total metal concentration of the nitrate electrolytes and the synthesis time allows to deposit Rh/Mg/Al hydrotalcite-like materials on FeCrAl fibers without pore blockage. Electrolytes with a low total metal concentration generate a compact coating in short time, while a high metal concentration could foster the deposition of Rh^0 and the development of a large number of cracks. Hence, the electrodeposition with diluted electrolytes can be a promising route to prepare materials for applications requiring low solid loading. Among several trials to adjust the deposition conditions in the concentration range of 0.03 – 0.10 M and synthesis time from 250 to 1000 s, the sample prepared in a 0.05 M of Rh/Mg/Al electrolyte (Rh/Mg/Al = 5/70/25 a.r.) for 1000 s exhibited a good compromise between solid loading and quality of the coating. As a result, 61% CH_4 conversion and 82% CO and 54% H_2 selectivity were achieved feeding a concentrated gas mixture ($CH_4/O_2/N_2$ = 2/1/4 v/v) at T_{oven} = 750 ºC and GHSV = 351,000 h^{-1}. However, further improvements in the quality of the coating, such as the decrease of the number of cracks, at high coating loading are required. In addition, the catalytic activity could be improved in future work with an increase in the number of discs tested.

4. Experimental Section

Electrochemical studies and catalyst preparation: Discs of FeCrAl fibers (diameter 10 mm x thickness 1 mm) were cut from a commercial panel. Rh/Mg/Al hydrotalcite-like compounds were in situ coated on the fibers by one-step electrodeposition using a homemade double-

compartment flow electrochemical cell by FAVS Gnudi, using a potentiostat (Autolab, PGSTAT128N, Eco Chemie) with GPES software. The fiber disc was used as a working electrode (W.E.), while a saturated calomel and Pt coil were used as reference electrode (R.E.) and counter electrode (C.E.), respectively. Detailed information on the cell can be found elsewhere.[32] Prior to coating, the fibers were subsequently washed in acetone, water and then dried at 60 ºC for 24 h.

Electrochemical behaviour of FeCrAl fibers was studied by linear sweep voltammetry (LSV) with a scan rate of 1 mV s^{-1} in different electrolytes, namely 0.135 M KCl or KNO_3, 0.0675 M $Mg(NO_3)_2$, 0.045 M $Al(NO_3)_3$, and 0.06 M mixture of $Mg(NO_3)_2$ and $Al(NO_3)_3$ (Mg/Al = 3/1 atomic ratio or a.r.). It should be noted that nitrate concentrations were deliberately kept constant in different electrolytes to study the nitrate reduction.

The electrodeposition was carried out in a mixture of nitrate precursors of Rh/Mg/Al (Rh/Mg/Al = 5/70/25 a.r.) at -1.2 V vs SCE (saturated calomel electrode). Electrolyte concentration was varied in the 0.03 – 0.10 M range, while synthesis time was prolonged from 250 to 1000 s depending on the concentration. After the electrodeposition, the coated fibers were thoroughly washed with distilled water and dried at 40 ºC for 24 h. The samples were then calcined at 900 ºC for 12 h with a 10 ºC min^{-1} heating rate in a static oven.

Catalyst characterization: The properties of the coating (morphology and composition) were analyzed by scanning electronic microscopy coupled with energy dispersive spectrometry (SEM/EDS) using an EP EVO 50 Series Instrument (EVO ZEISS) equipped with an INCA X-act Penta FET® Precision EDS microanalysis and INCA Microanalysis Suite Software (Oxford Instruments Analytical) to provide images of the spatial variation of elements in a sample. The accelerating voltage was 20 kV and the spectra were collected for 60 s. As-prepared deposited, calcined and spent coated fibers were analyzed in 2 – 3 regions of interest. The coating thickness was estimated from SEM images where the cracks were present. Micro-Raman spectra were recorded using a Renishaw Raman Invia spectrometer

configured with a Leica DMLM microscope using Ar^+ laser source (λ = 514.5 nm, P_{out} = 30 mW considering the decrease in power due to the plasma filter). In each measurement, the laser power was set by 10 % of the source and the signal was accumulated by 4 individual spectra with an acquisition time of 10 s.

Catalytic test: CPO tests were performed at atmospheric pressure using a quartz reactor (i.d. 10.0 mm) with one disc of coated fibers. Prior to the tests, the catalyst was reduced *in situ* with 7.0 L h^{-1} of a H_2/N_2 mixture (1/1 v/v) at 750 ºC for 2 h. The activity of the catalysts was sequentially evaluated by two different reaction conditions, namely feeding a diluted and a concentrated feed ($CH_4/O_2/N_2$ = 2/1/20 and 2/1/4 v/v, respectively) at an oven temperature of 750ºC and a gas hourly space velocity (GHSV) of 351,000 h^{-1} calculated on the basis of the volume of one fiber disc (10 mm of diameter and 1 mm of thickness) and a total flow rate of 460 mL min^{-1}. It should be remarked that the catalysts were tested with ratio O_2/CH_4 equal to 0.5, which does not help to avoid carbon deposits, indeed in the literature a slight excess of O_2 is feed to prevent carbon formation.[43,44] The temperature at the top of the fiber disc was measured by a K-type thermal couple inserted inside a two-milimeter quartz thermo-well in contacting with the fiber disc. Note that the temperature at the entrance of the fiber disc was higher than that of oven temperature depending on samples, e.g. 10-20 ºC and 50-100 ºC in diluted and concentrated gas mixture, respectively. Additionally, considering the mass of coating around 1.0 – 2.2 mg (for 0.03 M – 750 s and 0.10 M – 500 s, respectively), weight hourly space velocity (WHSV) was also calculated, being in the range of $1.25*10^7$ – $2.76*10^7$ L $kg_{coating}^{-1}$ h^{-1}. Control tests with diluted feed were carried out after the tests in concentrated conditions to check deactivation/activation processes. The effluent products were analyzed *on-line* after water condensation by a PerkinElmer Autosystem XL gas chromatograph, equipped with two TCDs and two Carbosphere columns using He as a carrier gas for CH_4, O_2, CO, and CO_2 measurements, and N_2 for H_2 analysis. Oxygen conversion was complete in all

tests. CH_4 and O_2 conversion and the selectivity in H_2 and CO were calculated as reported elsewhere.[46]

Supporting Information
Supporting Information is available from the Wiley Online Library.

Acknowledgements
P. H. Ho thanks to SINCHEM grant for Ph.D. research fellowship. SINCHEM is a joint-doctorate programme selected under Erasmus Mundus Action 1 programme (FPA 2013-0037). The financial support from the University of Bologna (FARB) is also acknowledged.

Received: ((will be filled in by the editorial staff))
Revised: ((will be filled in by the editorial staff))
Published online: ((will be filled in by the editorial staff))

References

[1] T.V. Choudhary, V.R. Choudhary, *Angew. Chem. Int. Ed.* **2008**, 47, 1828.

[2] H.A. Wright, J.D. Allison, D.S. Jack, G.H. Lewis, S.R. Landis, *Prepa. Pap. Am. Chem. Soc.*, *Div. Fuel Chem.* **2003**, 48, 2.

[3] L.E. Basini, A. Guarinoni, *Ind. Eng. Chem. Res.* **2013**, 52,17023.

[4] A. Donazzi, A. Beretta, G. Groppi, P. Forzatti, *J. Catal.* **2008**, 255, 241.

[5] R. Horn, K.A. Williams, N.J. Degenstein, A. Bitsch-Larsen, D. Dalle Nogare, S.A. Tupy, L.D. Schmidt, *J. Catal.* **2007**, 249, 380.

[6] C.Y. Zhao, *Int. J. Heat Mass Transfer* **2012**, 55, 3618.

[7] A. Montebelli, C.G. Visconti, G. Groppi, E. Tronconi, C. Cristiani, C. Ferreira, S. Kohler, *Catal. Sci. Technol.* **2014**, 4, 2846.

[8] E. Tronconi, G. Groppi, C.G. Visconti, *Curr. Opin. Chem. Eng.* **2014**, 5, 55.

[9] S. Cimino, L. Lisi, G. Russo, R. Torbati, *Catal. Today* **2010**, 154, 283.

[10] A. Beretta, A. Donazzi, D. Livio, M. Maestri, G. Groppi, E. Tronconi, P. Forzatti, *Catal. Today* **2011**, 171, 79.

[11] S. Cimino, G. Mancino, L. Lisi, *Appl. Catal. B Environ.* **2013**, 138-139, 342.

[12] A. Donazzi, D. Livio, A. Beretta, G. Groppi, P. Forzatti, *Appl. Catal. A Gen.* **2011**, 402, 41.

[13] R. Horn, K. Williams, N. Degenstein, L. Schmidt, *J. Catal.* **2006**, 242, 92.

[14] S. Ding, Y. Yang, Y. Jin, Y. Cheng, *Ind. Eng. Chem. Res.* **2009**, 48, 2878.

[15] A. Donazzi, M. Maestri, B.C. Michael, A. Beretta, P. Forzatti, G. Groppi, E. Tronconi, L.D. Schmidt, D.G. Vlachos, *J. Catal.* **2010**, 275, 270.

[16] P. Benito, G. Nuyts, M. Monti, W. De Nolf, G. Fornasari, K. Janssens, E. Scavetta, A. Vaccari, *Appl. Catal. B Environ.* **2015**, 179, 321.

[17] P. Benito, W. de Nolf, G. Nuyts, M. Monti, G. Fornasari, F. Basile, K. Janssens, F. Ospitali, E. Scavetta, D. Tonelli, A. Vaccari, *ACS Catal.* **2014**, 4, 3779.

[18] Y. Li, Y. Li, Q. Yu, L. Yu, *Catal. Commun.* **2012**, 29, 127.

[19] G. Groppi, E. Tronconi, G. Bozzano, M. Dente, *Chem. Eng. Sci.* **2010**, 65, 392.

[20] R. Chai, P. Chen, Z. Zhang, G. Zhao, Y. Liu, Y. Lu, *Catal. Commun.* **2017**, 101, 48.

[21] Y. Ma, Y. Ma, Z. Zhao, X. Hu, Z. Ye, J. Yao, C.E. Buckley, D. Dong, *Renew. Energ.* **2019**, 138, 1010.

[22] R. Chai, G. Zhao, Z. Zhang, P. Chen, Y. Liu, Y. Lu, *Catal. Sci. Technol.* **2017**, 7, 5500.

[23] R. Chai, S. Fan, Z. Zhang, P. Chen, G. Zhao, Y. Liu, Y. Lu, *ACS Sustain. Chem. Eng.* **2017**, 5, 4517.

[24] P. Fornasiero, T. Montini, M. Graziani, S. Zilio, M. Succi, *Catal. Today* **2008**, 137, 475.

[25] H. Li, Y. Wang, X. Chen, S. Liu, Y. Zhou, Q. Zhu, Y. Chen, H. Lu, *RSC Adv.* **2018**, 8, 14806.

[26] I.V. Lukiyanchuk, V.S. Rudnev, M.M. Serov, B.L. Krit, G.D. Lukiyanchuk, P.M. Nedozorov, *Appl. Surf. Sci.* **2018**, 436, 1.

[27] E. Reichelt, M. Jahn, *Chem. Eng. J.* **2017**, 325, 655.

[28] E. Reichelt, M.P. Heddrich, M. Jahn, A. Michaelis, *Appl. Catal. A Gen.* **2014**, 476, 78.

[29] P.H. Ho, M. Ambrosetti, G. Groppi, E. Tronconi, R. Palkovits, G. Fornasari, A. Vaccari, P. Benito, in Studies in Surface Science and Catalysis (Eds. S. Albonetti, S. Perathoner, E.A. Quadrelli), Elsevier **2019**, Ch. 15.

[30] P. Benito, F. Basile, G. Fornasari, M. Monti, E. Scavetta, D. Tonelli, A. Vaccari, in *New Strategies in Chemical Synthesis and Catalysis* (Ed. B. Pignataro), Wiley **2012**, Ch. 9.

[31] P. Benito, M. Monti, I. Bersani, F. Basile, G. Fornasari, E. Scavetta, D. Tonelli, A. Vaccari, *Catal. Today* **2012**, 197, 162.

[32] P.H. Ho, W. de Nolf, F. Ospitali, A. Gondolini, G. Fornasari, E. Scavetta, D. Tonelli, A. Vaccari, P. Benito, *Appl. Catal. A Gen.* **2018**, 560, 12.

[33] P.H. Ho, M. Ambrosetti, G. Groppi, E. Tronconi, J. Jaroszewicz, F. Ospitali, E. Rodríguez-Castellón, G. Fornasari, A. Vaccari, P. Benito, *Catal. Sci. Technol.* **2018**, 8, 4678.

[34] P.H. Ho, M. Ambrosetti, G. Groppi, E. Tronconi, G. Fornasari, A. Vaccari, P. Benito, *Catal. Today* **2019**, 334, 37.

[35] M.A. Vuurman, D.J. Stufkens, A. Oskam, J.A. Moulijn, F. Kapteijn, *J. Mol. Catal.* **1990**, 60, 83.

[36] D. Zhang, W. Choi, Y. Oshima, U. Wiedwald, S.H. Cho, H.P. Lin, Y.K. Li, Y. Ito, K. Sugioka, *Nanomaterials* **2018**, 8, 631.

[37] D.L.A. de Faria, F.N. Lopes, *Vib. Spectrosc.* **2007**, 45, 117.

[38] C. Cionea, M.D. Abad, Y. Aussat, D. Frazer, A.J. Gubser, P. Hosemann, *Sol. Energy Mater. Sol. Cells* **2016**, 144, 235.

[39] P.H. Ho, M. Monti, E. Scavetta, D. Tonelli, E. Bernardi, L. Nobili, G. Fornasari, A. Vaccari, P. Benito, *Electrochim. Acta* **2016**, 222, 1335.

[40] P.H. Ho, E. Scavetta, F. Ospitali, D. Tonelli, G. Fornasari, A. Vaccari, P. Benito, *Appl. Clay Sci.* **2018**, 151, 109.

[41] P. Benito, M. Monti, W. De Nolf, G. Nuyts, G. Janssen, G. Fornasari, E. Scavetta, F. Basile, K. Janssens, F. Ospitali, D. Tonelli, A. Vaccari, *Catal. Today* **2015**, 246, 154.

[42] P.H. Ho, W. De Nolf, F. Ospitali, D. Beton, L. Torkuhl, G. Fornasari, A. Vaccari, P. Benito, *React. Chem. Eng.* **2019**, 4, 1768.

[43] A. Beretta, G. Groppi, M. Lualdi, I. Tavazzi, P. Forzatti, *Ind. Eng. Chem. Res.* **2009**, 48, 3825.

[44] T. Bruno, A. Beretta, G. Groppi, M. Roderi, P. Forzatti, *Catal. Today* **2005**, 99, 89.

[45] S. Specchia, G. Negro, G. Saracco, V. Specchia, *Appl. Catal. B* **2007**, 70, 525.

[46] A. Ballarini, P. Benito, G. Fornasari, O. Scelza, A. Vaccari, *Int. J. Hydrog. Energy* **2013**, 38, 15128.

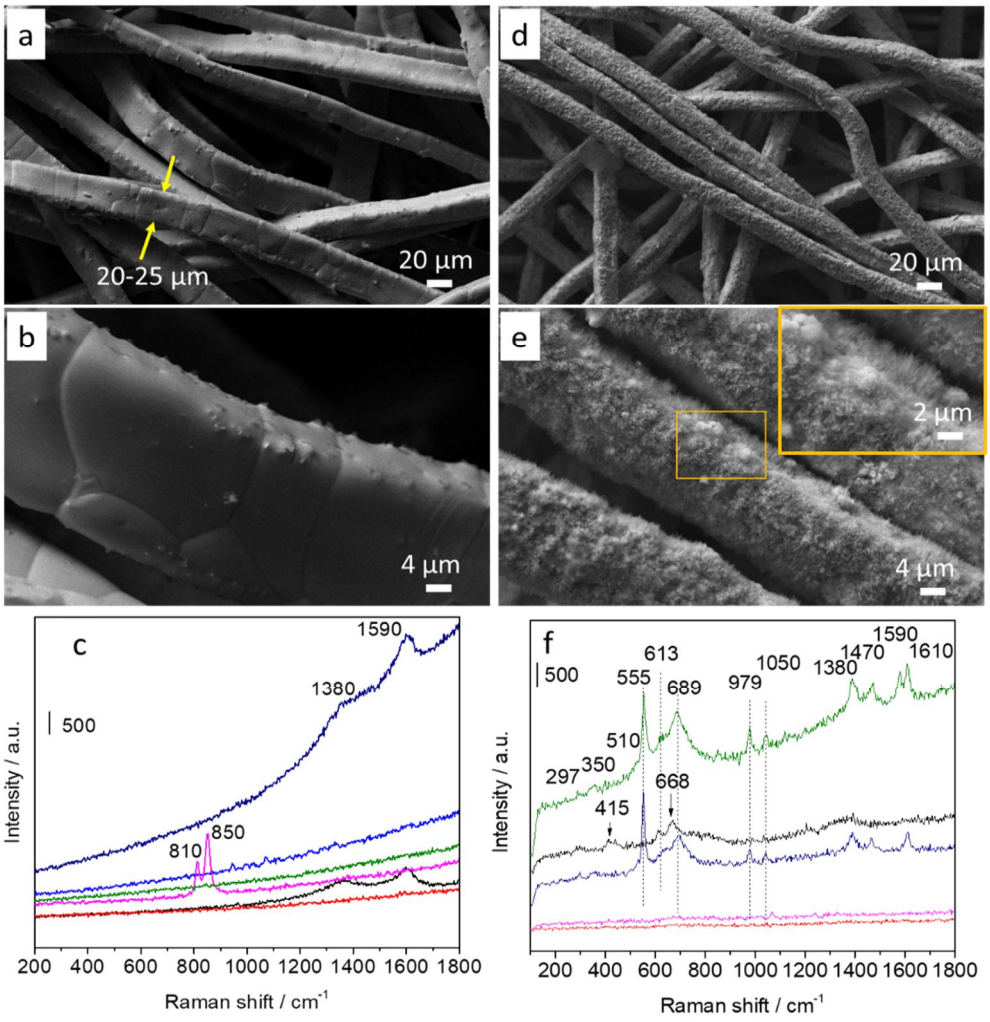

Figure 1. Characterization of bare fiber before and after calcination at 900 ºC for 12 h: a and b) SEM images and c) Raman spectrum of fresh fiber; d and e) SEM images and f) Raman spectrum of calcined fiber.

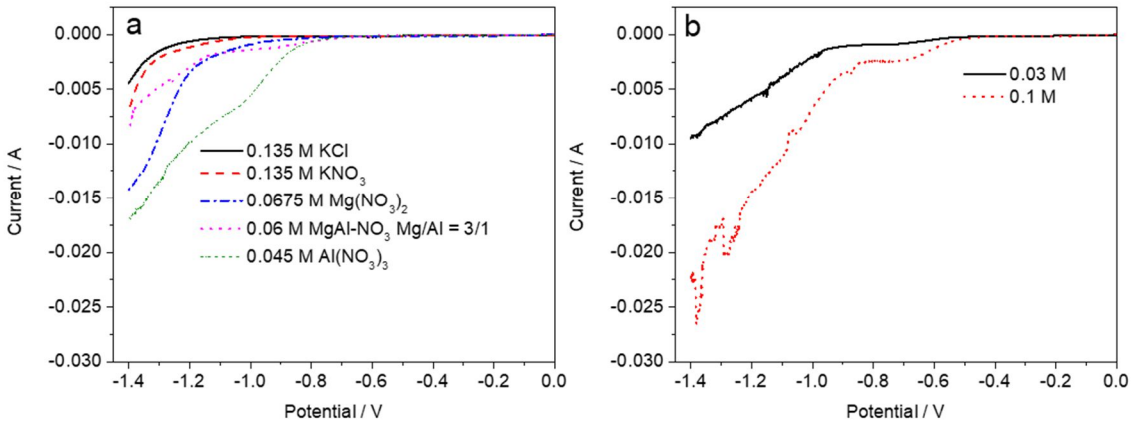

Figure 2. Linear sweep voltammetry of FeCrAl fibers in various electrolytes: a) absence of Rh and b) presence of Rh (Rh/Mg/Al = 5/70/25 a.r.). Scan rate 1 mV s^{-1}, from 0 to -1.4 V vs SCE.

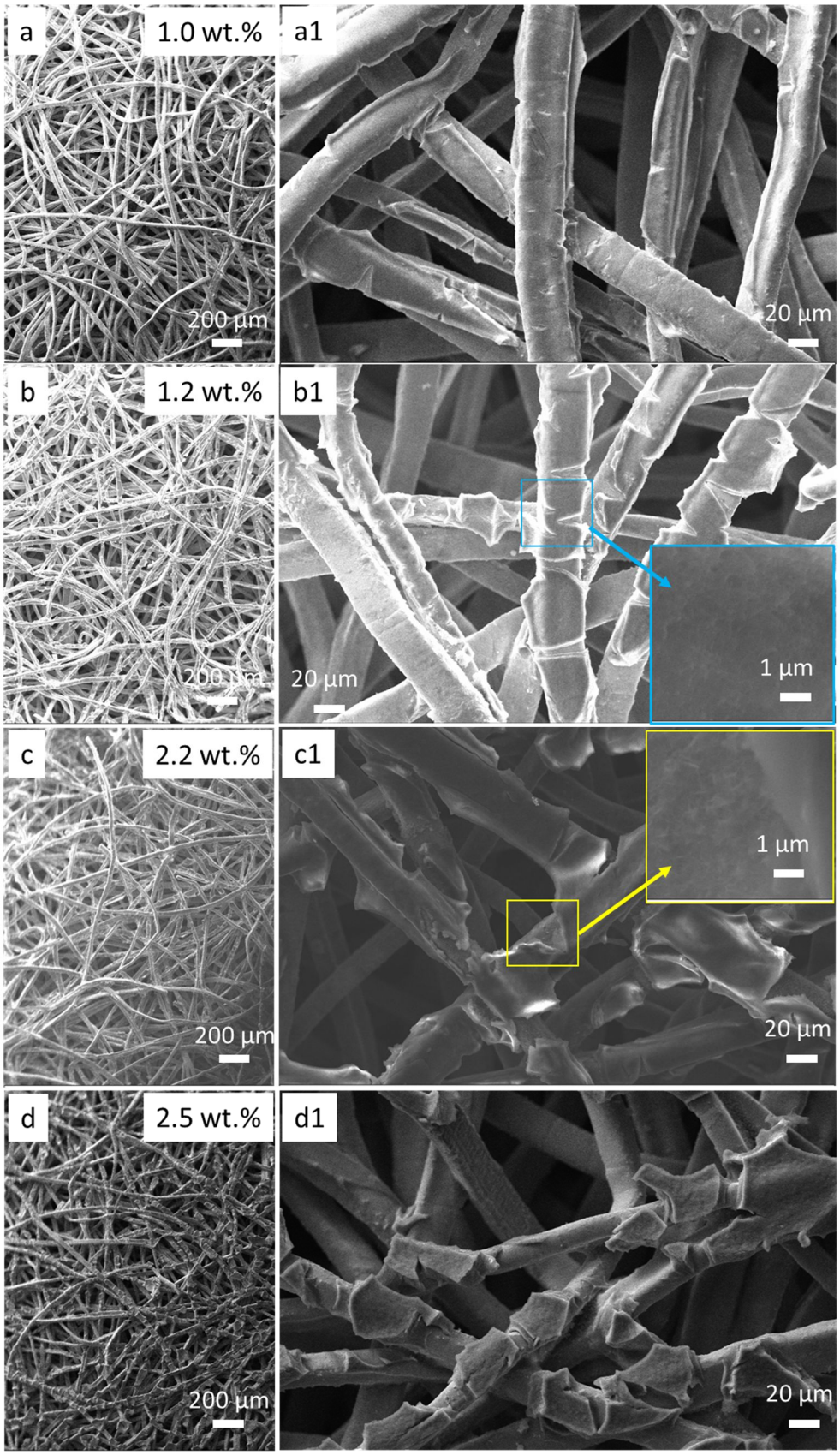

Figure 3. SEM images of electrodeposited samples of fibers in 0.06 M RhMgAl electrolytes at -1.2 V vs SCE for different synthesis time: 250 s (a, a1), 500 s (b, b1), 750 s (c, c1), and 1000 s (d, d1).

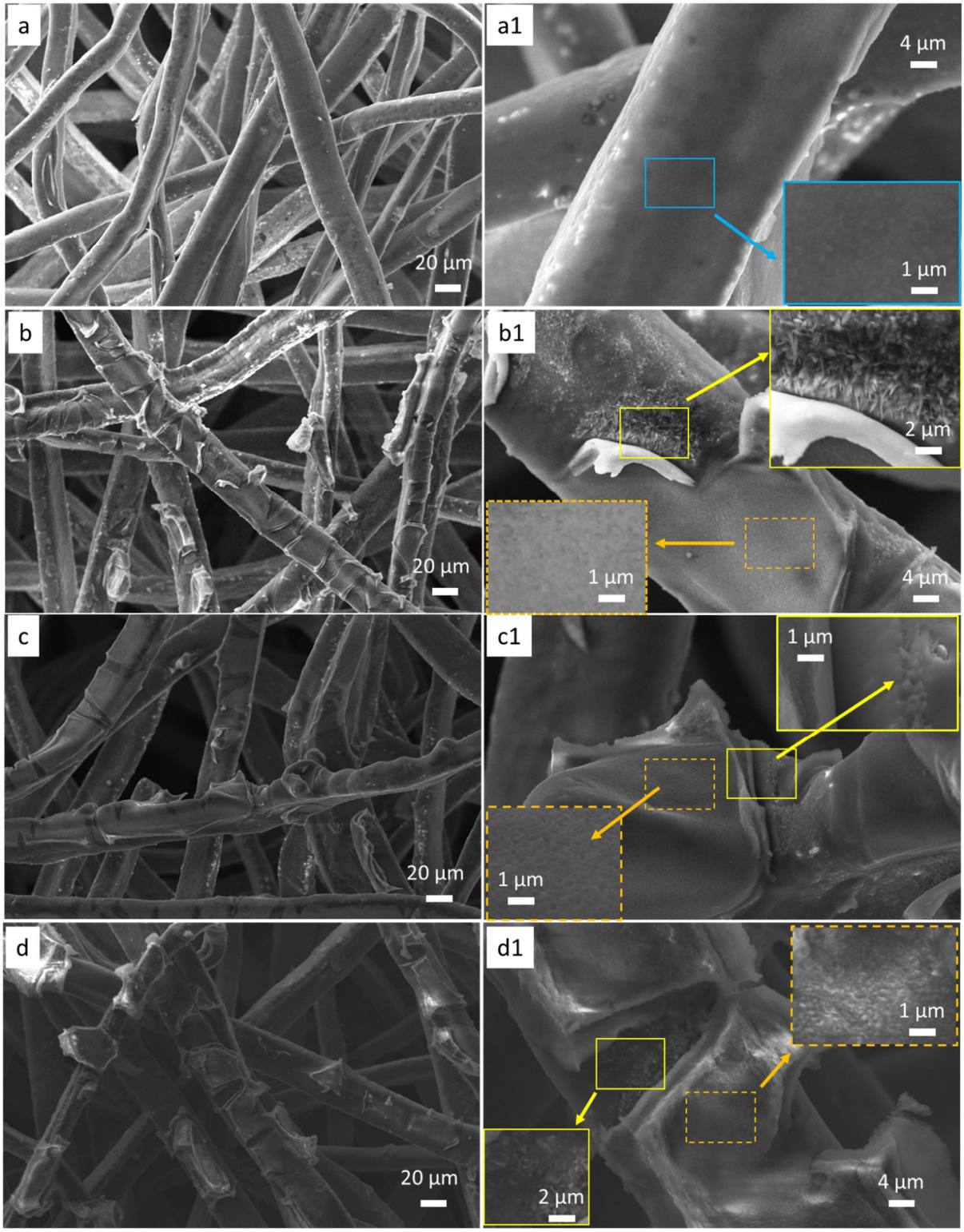

Figure 4. SEM images of fibers prepared in 0.06 M RhMgAl electrolytes at -1.2 V vs SCE for different synthesis time, followed by calcination at 900 ºC for 12 h, and temperature ramp of 10 ºC min^{-1}: 250 s (a, a1), 500 s (b, b1), 750 s (c, c1), and 1000 s (d, d1).

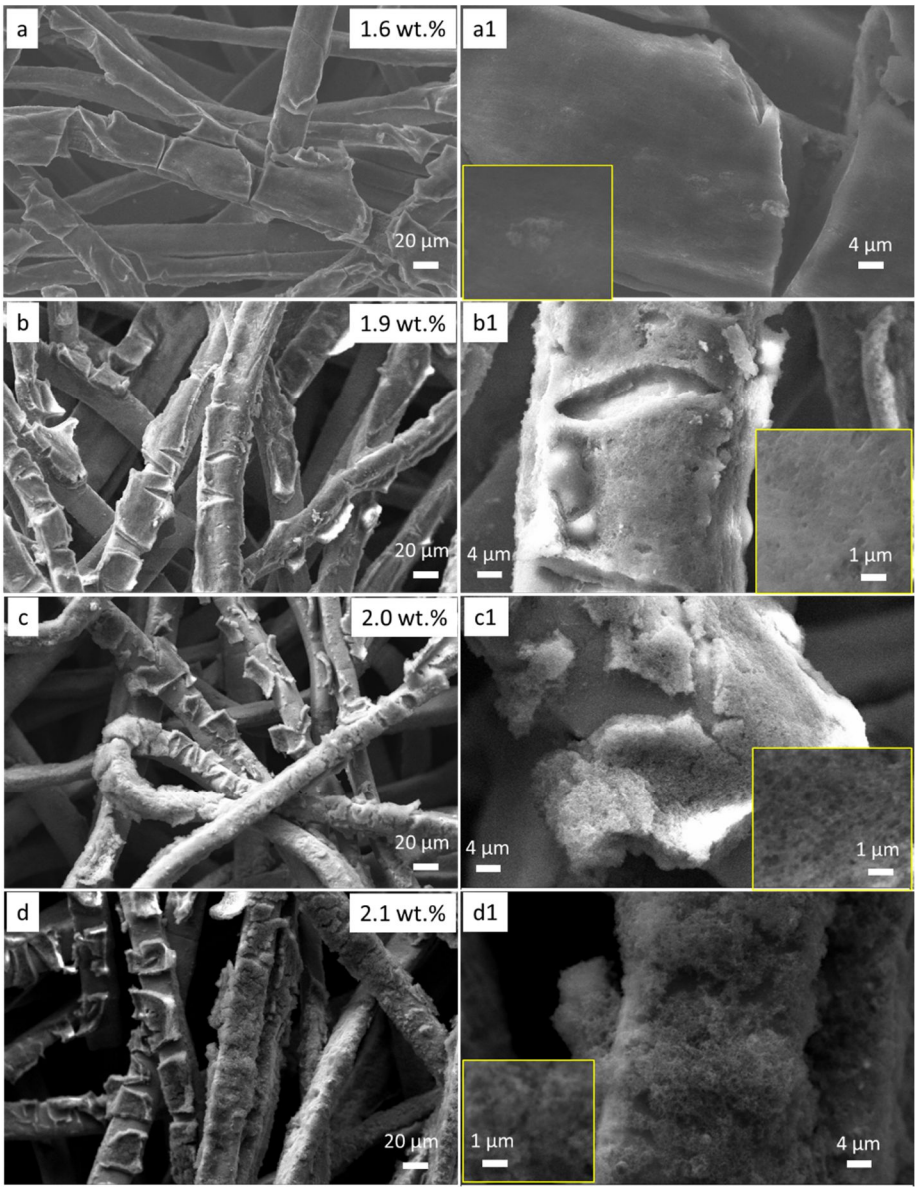

Figure 5. SEM images of electrodeposited samples of fibers at -1.2 V vs SCE at different synthesis conditions: 0.03 M – 750 s (a, a1), 0.03 M - 1000 s (b, b1), 0.05 M - 750 s (c, c1), and 0.05 M - 1000 s (d, d1).

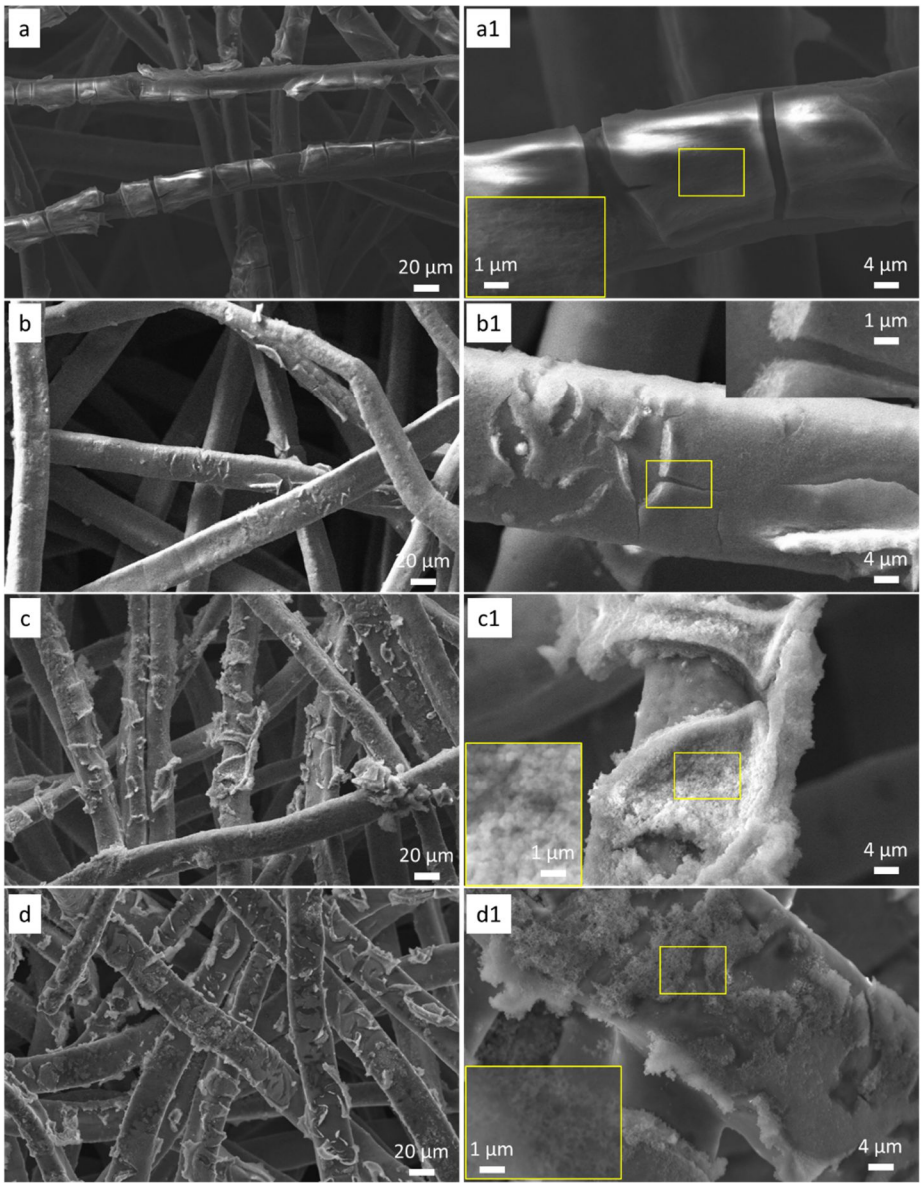

Figure 6. SEM images of calcined samples of covered fibers prepared at -1.2 V vs SCE at different synthesis conditions followed by calcination at 900 ºC for 12 h and temperature ramp of 10 ºC min^{-1}: 0.03 M – 750 s (a, a1), 0.03 M - 1000 s (b, b1), 0.05 M - 750 s (c, c1), and 0.05 M - 1000 s (d, d1).

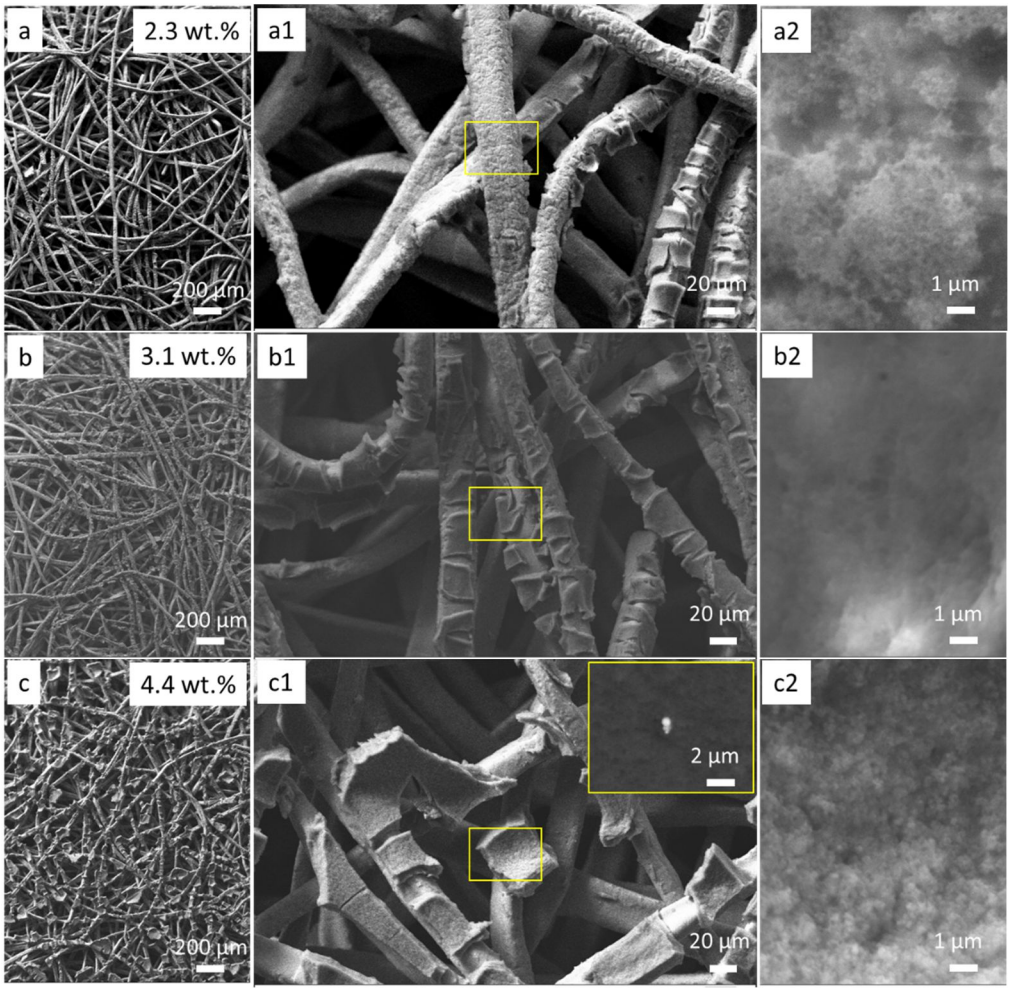

Figure 7. SEM images of electrodeposited samples on fibers prepared in 0.1 M Rh/Mg/Al electrolytes at -1.2 V vs SCE at different synthesis times: 250 s (a, a1, a2), 350 s (b, b1, b2), 500 s (c, c1, c2).

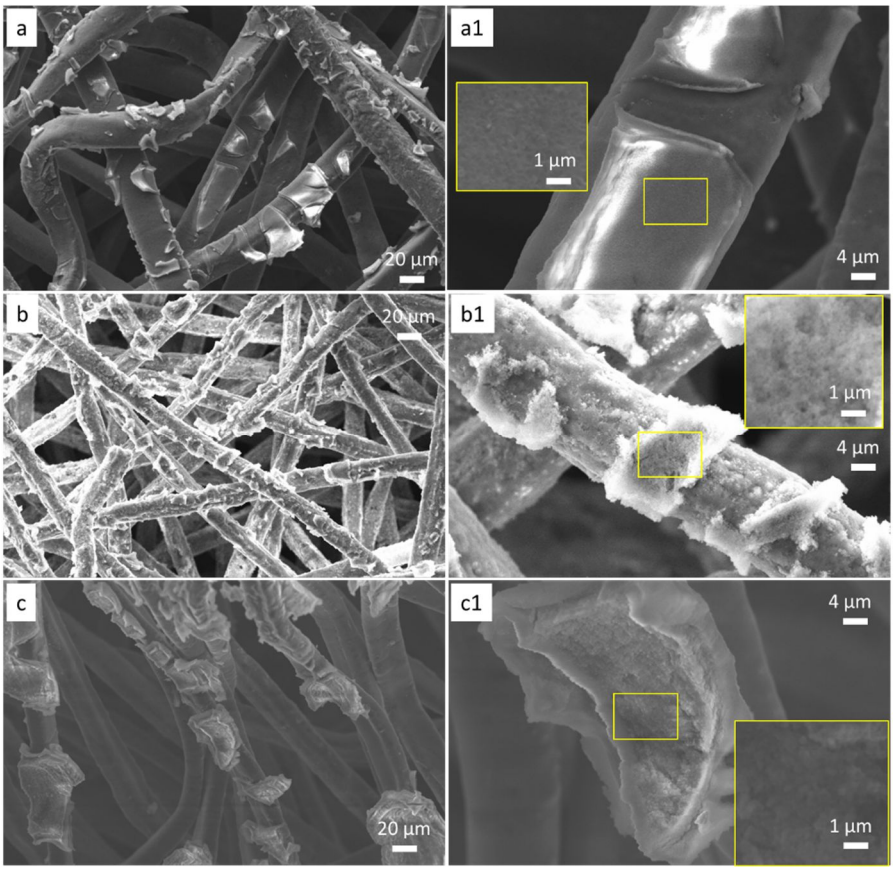

Figure 8. SEM images of calcined samples prepared in 0.1 M Rh/Mg/Al electrolytes at -1.2 V vs SCE at different synthesis times and following calcination at 900 ºC for 12 h with a temperature ramp of 10 ºC min^{-1}: 250 s (a, a1), 350 s (b, b1), 500 s (c, c1).

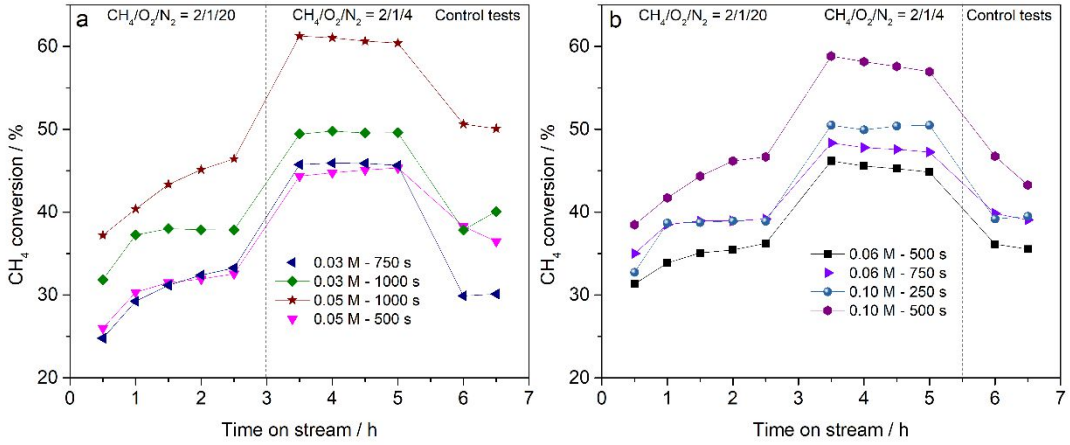

Figure 9. Catalytic activity tests for fiber structured catalysts prepared at a) low concentration and b) high concentration of electrolytes. T_{oven} = 750 ºC and GHSV = 351,000 h^{-1}. Note that depending on samples the temperature at the entrance of the fiber disc was higher than that of oven temperature, e.g. 10-20 ºC and 50-100 ºC in diluted and concentrated gas mixture, respectively.

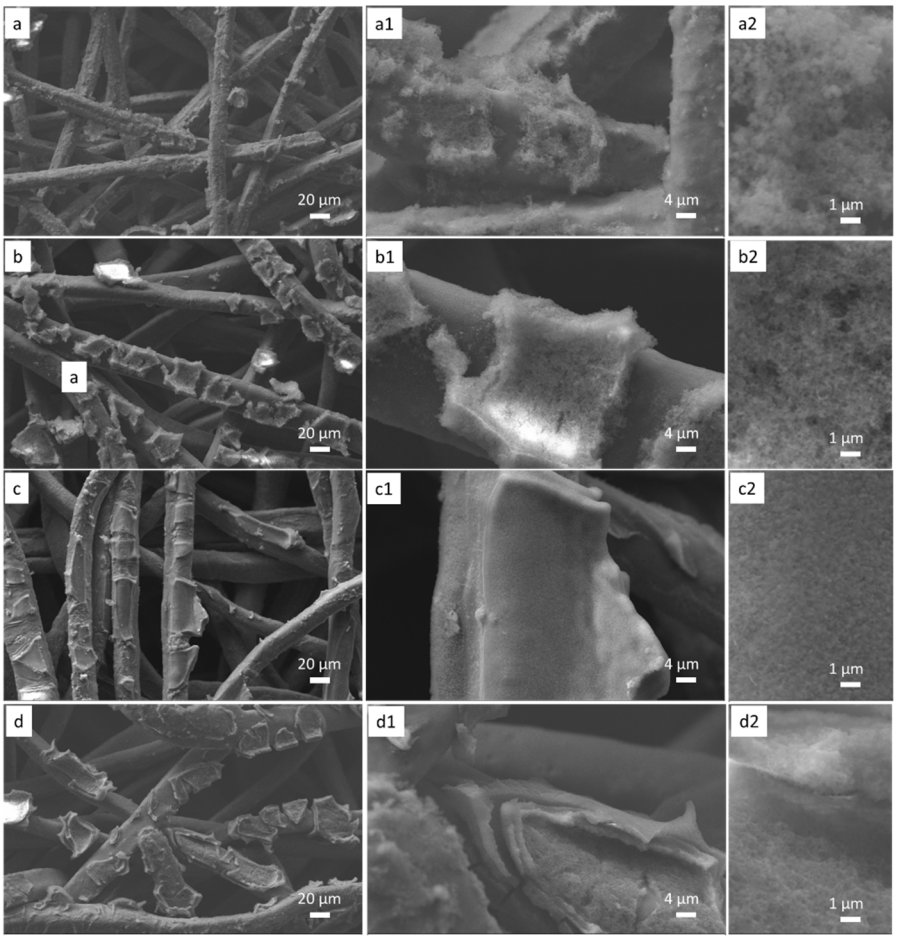

Figure 10. SEM images of spent catalysts prepared at different synthesis conditions: 0.03 M – 1000 s (a, a1, a2), 0.05 M - 1000 s (b, b1, b2), 0.06 M - 750 s (c, c1, c2), and 0.10 M - 500 s (d, d1, d2).

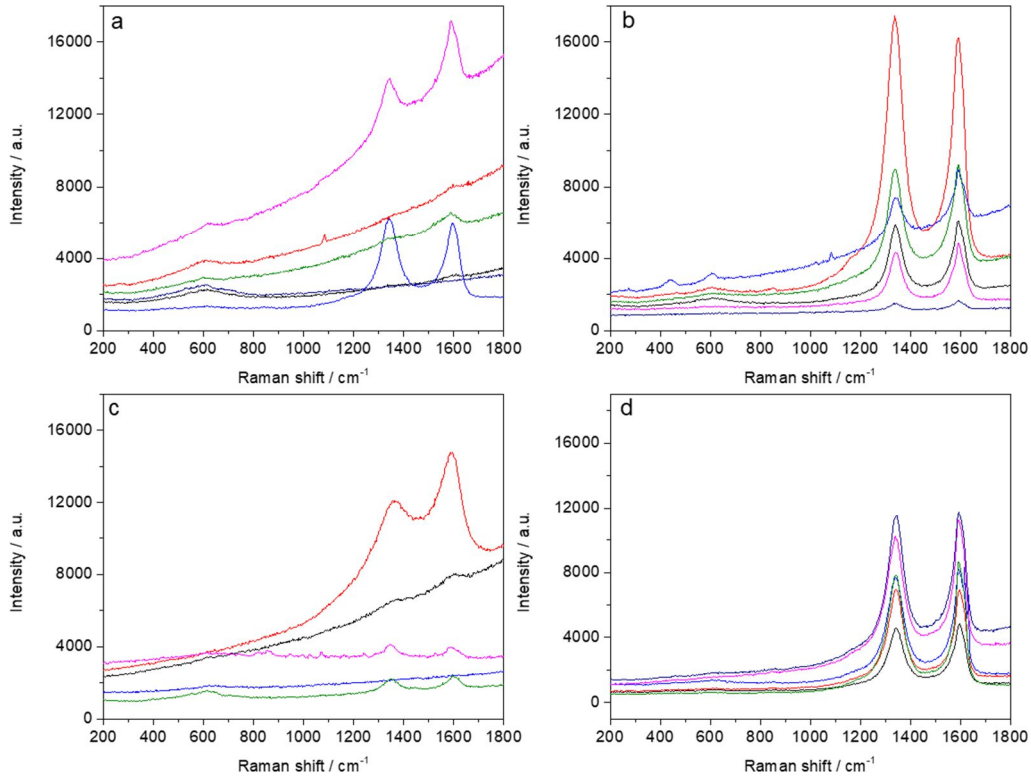

Figure 11. Raman characterization for selected spent catalysts: a) 0.03 M – 1000 s, b) 0.05 M – 1000 s, c) 0.06 M – 750 s, and d) 0.1 M – 500 s).

Table 1. Average CH_4 conversion, CO and H_2 selectivity and H_2/CO mole ratio of syngas production on various fiber structured catalysts prepared at different synthesis conditions. Reaction conditions: one coated disc, GHSV = 351,600 h^{-1}, T_{oven} = 750 ºC, $CH_4/O_2/N_2$ = 2/1/20 (diluted) or 2/1/4 v/v (concentrated feedstock). Average values were calculated from four analyses for each reaction condition

Sample	Conversion (%)	CO Sel. (%)	H_2 Sel. (%)	H_2/CO (molar ratio)
0.03 M – 750 s	32.3 ± 1.0	56.2 ± 1.7	10.6 ± 0.5	0.38 ± 0.01
	45.8 ± 0.1	*83.9 ± 0.7*	*25.7 ± 0.6*	*0.61 ± 0.02*
0.03 M – 1000 s	37.7 ± 0.4	55.1 ± 1.8	14.0 ± 1.1	0.51 ± 0.04
	49.6 ± 0.1	*83.2 ± 0.4*	*33.7 ± 0.2*	*0.81 ± 0.01*
0.05 M – 500 s	31.6 ± 0.8	61.8 ± 0.4	11.1 ± 0.5	0.36 ± 0.02
	44.9 ± 0.4	*84.4 ± 0.1*	*21.1 ± 1.1*	*0.50 ± 0.03*
0.05 M – 1000 s	45.0 ± 1.5	65.4 ± 2.9	31.5 ± 3.4	0.96 ± 0.06
	60.8 ± 0.4	*82.2 ± 0.2*	*54.4 ± 0.8*	*1.32 ± 0.02*
0.06 M – 500 s	35.6 ± 0.6	63.1 ± 1.4	16.4 ± 1.0	0.52 ± 0.02
	45.5 ± 0.6	*79.7 ± 1.0*	*30.4 ± 1.3*	*0.76 ± 0.03*
0.06 M – 750 s	39.0 ± 0.2	61.3 ± 1.0	16.4 ± 0.5	0.53 ± 0.01
	47.7 ± 0.5	*78.9 ± 1.0*	*31.5 ± 1.5*	*0.79 ± 0.04*
0.10 M – 250 s	38.9 ± 0.1	67.1 ± 0.4	14.2 ± 0.5	0.42 ± 0.02
	50.3 ± 0.3	*84.5 ± 0.9*	*35.9 ± 0.7*	*0.85 ± 0.01*
0.10 M – 500 s	45.7 ± 1.2	73.6 ± 1.2	31.1 ± 1.6	0.85 ± 0.03
	57.9 ± 0.8	*84.4 ± 0.5*	*50.1 ± 1.5*	*1.19 ± 0.03*

[a] For each sample, the second line with italic letters shows data in concentrated feedstock.

Electro-base generation method is effective to coat FeCrAl fiber without pore blockage. It is a promising alternative to dip-coating for the preparation of structured catalysts based on metallic fiber supports.

Keyword structured catalysts, electrodeposition; hydrotalcite-like materials, FeCrAl fibers, catalytic partial oxidation of methane

Phuoc Hoang Ho, Francesca Ospitali, Giancosimo Sanghez De Luna, Giuseppe Fornasari, Angelo Vaccari, and Patricia Benito*

On the coating of Rh/Mg/Al hydrotalcite-like materials on FeCrAl fibers by electrodeposition and application for syngas production

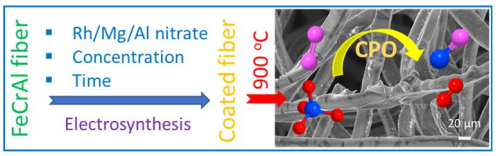

Supporting Information

On the coating of Rh/Mg/Al hydrotalcite-like materials on FeCrAl fibers by electrodeposition and application for syngas production

*Phuoc Hoang Ho, Francesca Ospitali, Giancosimo Sanghez De Luna, Giuseppe Fornasari, Angelo Vaccari, and Patricia Benito**

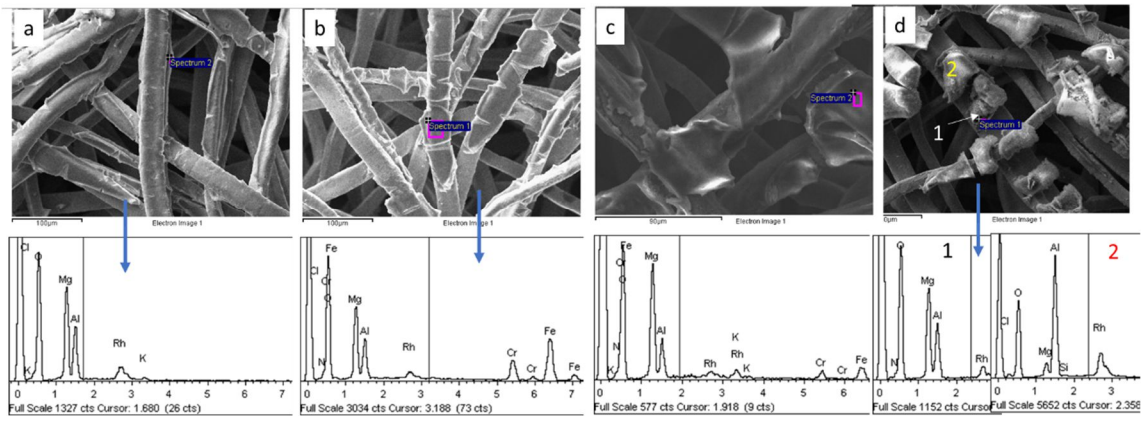

Figure S1. SEM images and respective EDS spectra of the fibers prepared in 0.06 M electrolyte of RhMgAl nitrate mixture at -1.2 V vs SCE for different synthesis time: (a) 250 s; (b) 500 s; (c) 750 s; and (d) 1000 s.

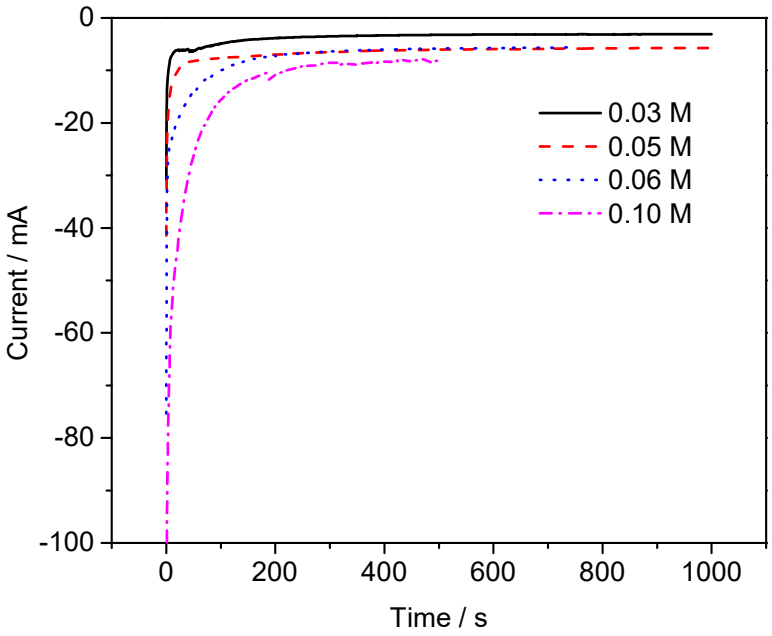

Figure S2. Effect of total metal concentration on transition curves of current during the electrodeposition.

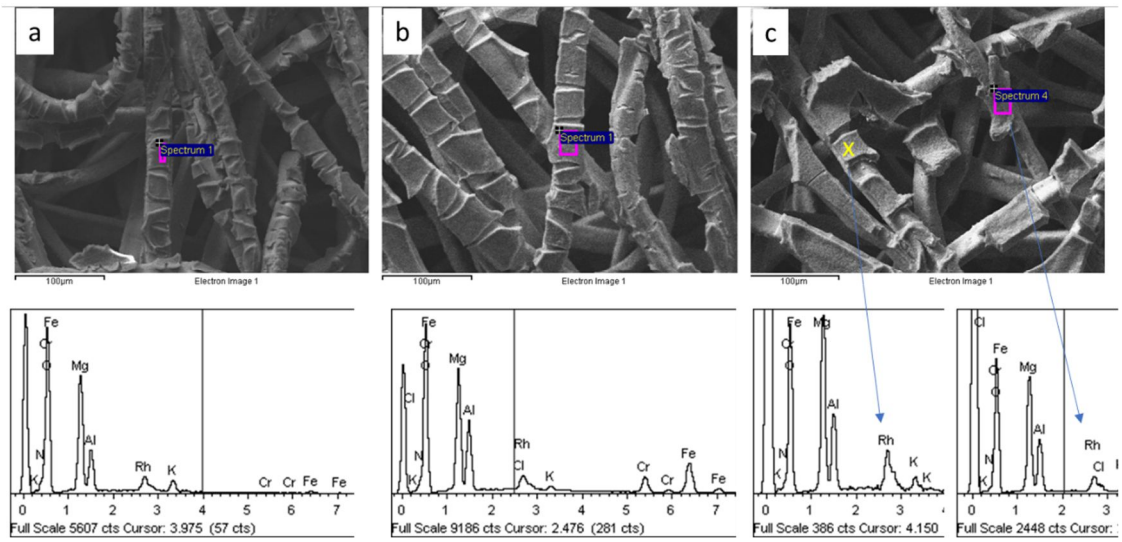

Figure S3. SEM images and respective EDS spectra of the fibers prepared in 0.1 M electrolyte of RhMgAl nitrate mixture at -1.2 V vs SCE for different synthesis time: (**a**) 250 s; (**b**) 350 s; and (c) 500 s. Location marked with yellow symbol (X) in Figure (c) showed presence of Rh metallic particle which could be observed in the inset of Figure 5 c1.

Supporting Information

Coating of Rh/Mg/Al hydrotalcite-like materials on FeCrAl fibers by electrodeposition and application for syngas production

*Phuoc Hoang Ho, Francesca Ospitali, Giancosimo Sanghez De Luna, Giuseppe Fornasari, Angelo Vaccari, and Patricia Benito**

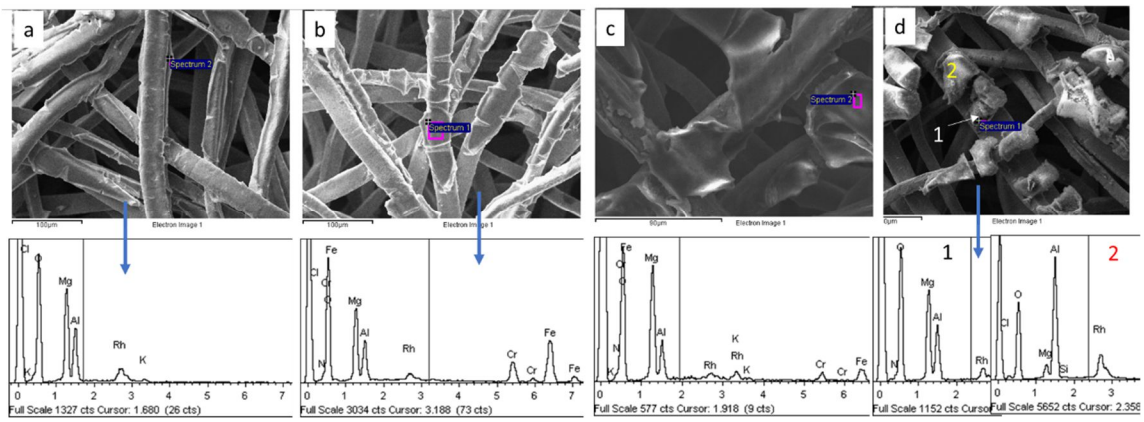

Figure S1. SEM images and respective EDS spectra of the fibers prepared in 0.06 M electrolyte of RhMgAl nitrate mixture at -1.2 V vs SCE for different synthesis time: (a) 250 s; (b) 500 s; (c) 750 s; and (d) 1000 s.

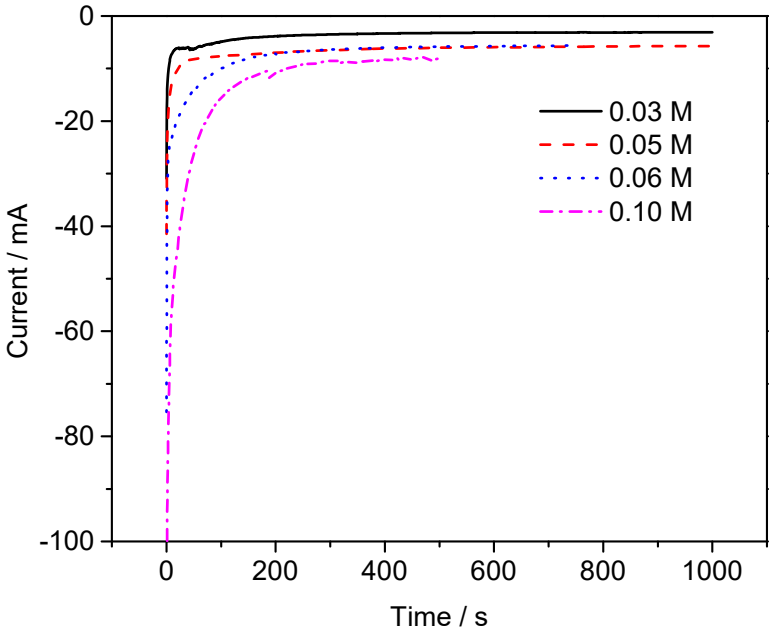

Figure S2. Effect of total metal concentration on transition curves of current during the electrodeposition.

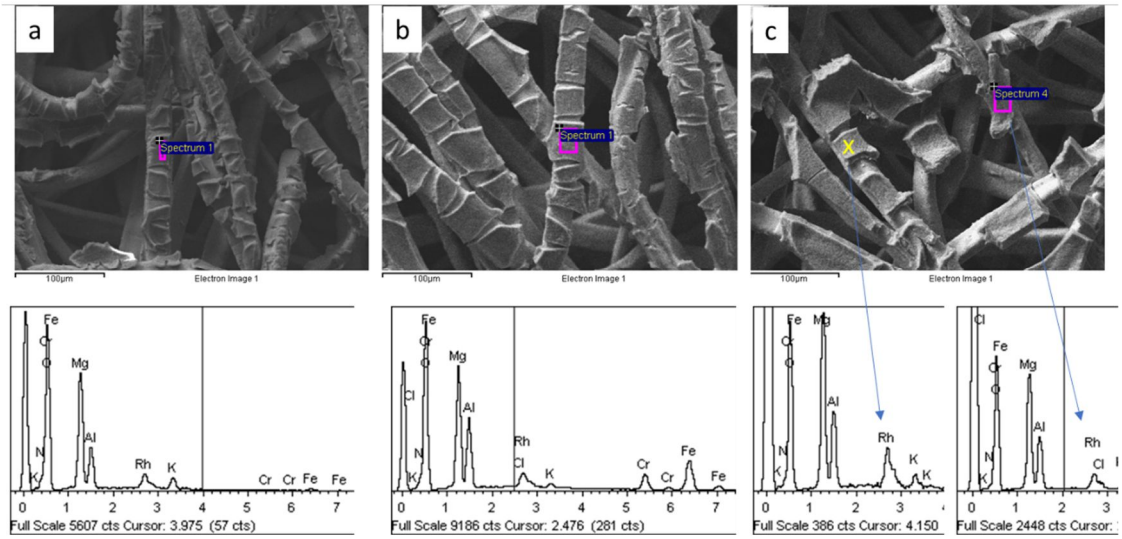

Figure S3. SEM images and respective EDS spectra of the fibers prepared in 0.1 M electrolyte of RhMgAl nitrate mixture at -1.2 V vs SCE for different synthesis time: (**a**) 250 s; (**b**) 350 s; and (c) 500 s. Location marked with yellow symbol (X) in Figure (c) showed presence of Rh metallic particle which could be observed in the inset of Figure 5 c1.